HEALTH MANAGEMENT USING FAULT DETECTION AND FAULT TOLERANT CONTROL OF MULTICELLULAR CONVERTER APPLIED IN MORE ELECTRIC AIRCRAFT SYSTEM

Mohamed Abdelbasset MAHBOUB, Boubakeur ROUABAH ⬤, Mohamed Redouane KAFI, Houari TOUBAKH

Kasdi Merbah Ouargla University, Algeria
* Corresponding author, e-mail: boubakeurrouabah@yahoo.fr

Abstract

The increased cost of fuel and maintenance in aircraft system lead to the concept of more electric aircraft, moreover this concept increase the use of power electronic converters in aircraft power system. Since in this application, the reliability is a crucial feature. Therefore, the use of more efficient, reliable and robust power converter with health management capability will be a big challenge. Multicellular topology of power converters has the required performance in terms of efficiency and robustness. However, the increased complexity of control and more power components (power switches and capacitors) goes along with an increase in possibility of failure in multicellular topology. Therefore, the main contribution of this paper is the use of multicellular topology advantageous with fault diagnosis and fault tolerant control in order to increase the robustness reliability. The health management using a fault detection with Fuzzy Pattern Matching (FPM) algorithm when a failure in power switches or flying capacitors of multicellular converter and a Fault Tolerant Control (FTC) with sliding mode of second parallel three cells multicellular converters. Simulation results with Matlab show the increased efficiency and the continuity of work during failure mode in aircraft power system.

Keywords: fault tolerant control (FTC); multicellular converter; more electric aircraft

1. INTRODUCTION

Recently, the aircraft system plays an important role in globe world economics, human culture, space discovering, and technology development [1-2]. However, in order to obtain aircraft with fewer carbon emission, fuel saving, quitter flight and reduced weight and noise, the traditionally actuators powered by mechanical, pneumatic, and hydraulic sources such as environmental control, wing ice protection, and fuel pumping systems) are replaced by controlled electric systems [3-5]. To this manner, a considerable change in the design of modern aircraft. The planes Airbus A380 and Boeing 787 have more electrical systems compared with previous planes [6]. This increase of electric systems uses leads to the concept of more electric aircraft. Therefore, high voltage power electronic converters are enabling modern aircraft to adjust and control the electric loads. However, the transfer to new concept of more electric aircraft is challenged by strict requirements of safety and continuity of operation in its electrical power systems [7-9]. Therefore, the use of more efficient and robust power converter in more electric power system is necessary. Multicellular power converters or flying capacitor topology has more advantageous compared with other power converter topologies, such as reduced stress on power switches, high switching frequency capability and small dv/dt [10-12]. In [13-14] a multicellular converter shows a good robustness against parametric variations and current harmonics for a various control method. A simulation and experimental study shows good balancing of capacitor voltages and no interharmonics has been produced in multicellular converter. In [15], the robustness and stability are confirmed for multicellular converter. However, the multicellular topology present higher redundancy of power switches and flying capacitors, and because the aircraft systems need to guarantee the safety and the availability of operation, health management with fault diagnostics and fault tolerant control are necessary. A multicellular converter with fault diagnosis is used in order to enhance the performance of wind turbine system [16]. While, in [17], an approach based on the use of a machine Learning technique is developed to perform an early fault diagnosis method of power switches faults in wind turbine converters with hybrid dynamic classifier for multicellular converter in wind turbines is proposed. In [18] a fault diagnosis and fault

tolerant control of multicellular converter used in shunt active power filter in order to enhance the efficiency and the reliability of active filter, and advanced fault-tolerant control strategy of wind turbine based on squirrel cage induction generator with rotor bar defects in order to extend the lifetime of wind energy conversion system [19].

In electric system of aircraft, different fault diagnosis methods are used in literature. Diagnosis strategy of nonstationary (transient) states of direct current in electric power systems of aircraft [20]. In [21], a fault diagnosis method using acoustic signature of aircraft auxiliary power unit.

However, a Fuzzy Pattern Matching (FPM) algorithm is used in fault diagnosis as reduced time method of classification (the detection, integration and adaptation online) [22-24]

Therefore, the contribution of this paper is the use of FPM and multicellular topology advantageous in more electric aircrafts with more reliability and increased robustness. These can improve the efficiency and the safety of studied system.

This paper proposes a multicellular topology of two parallel converters with fault tolerant control and fault diagnosis using Fuzzy Pattern Matching (FPM) algorithm.

This paper is organized as follow: in section 2 modelling of proposed system than in section 3 presentation of Fuzzy Pattern Matching (FPM) algorithm, in section 4 simulation results with Matlab and finally conclusion in section 5.

Figure 1 shows the proposed system structure.

2. MODELING OF PROPOSED STRUCTURE

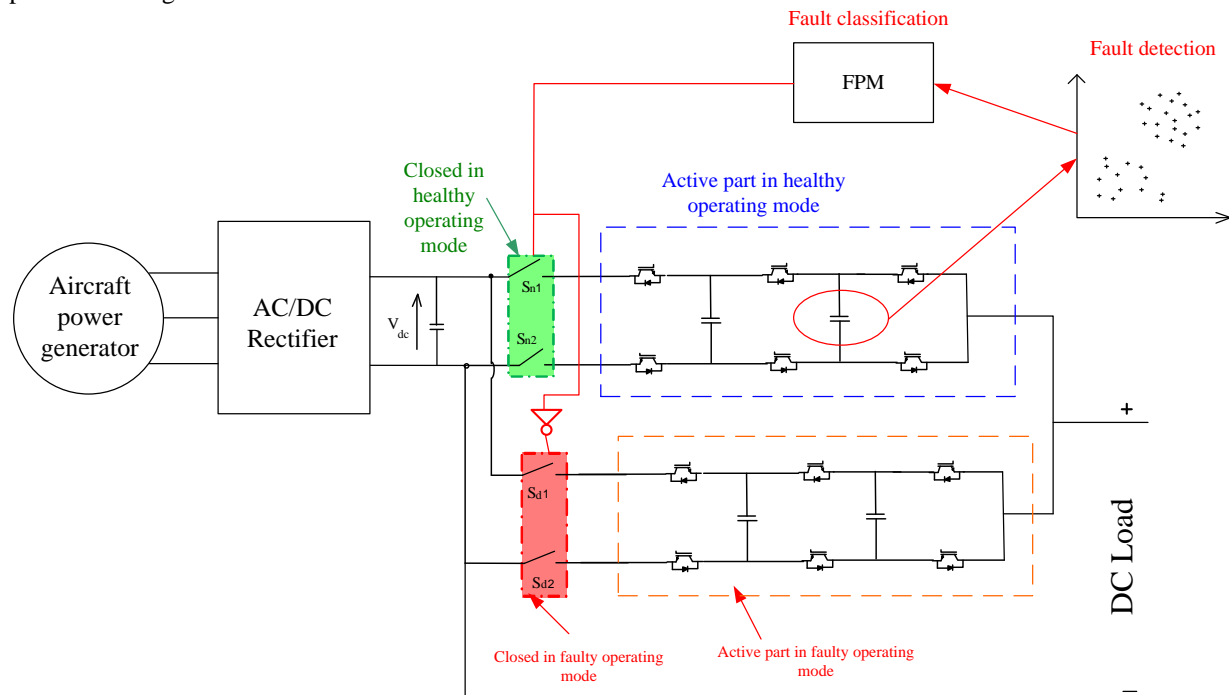The multicellular topology of power converter is presented in figure 2.

$$i_{Ci} = C_i \frac{d}{dt} V_{Ci} \tag{1}$$

$$\frac{d}{dt} V_{Ci} = \frac{1}{C_i} \left[S_{(i+1)} - S_i \right] i_L \tag{2}$$

i_{Ci} is the current of flying capacitor C_i
V_{Ci} means V_{C1} and V_{C2}

$$L_L \frac{di_L}{dt} = V_S - R_L i_L \tag{3}$$

$$V_S = S_1[V_{C1}] + S_2[V_{C2} - V_{C1}] + S_3[V_{dc} - V_{C2}] \tag{4}$$

$$\frac{di_L}{dt} = \frac{1}{L_L} (S_1[V_{C1}] + S_2[V_{C2} - V_{C1}] + S_3[V_{dc} - V_{C2}]) - R_L i_L \tag{5}$$

L_L and R_L are the resistor and inductor of electric load, S_1, S_2 and S_3 are the state of power switches.

The nonlinear model of multicellular converter topology used in photovoltaic system is given by Equation (6).

$$\begin{bmatrix} \dot{V}_{C1} \\ \dot{V}_{C2} \\ i_L \end{bmatrix} = \begin{bmatrix} 0 & 0 & 0 \\ 0 & 0 & 0 \\ 0 & 0 & \frac{-R_L}{L_L} \end{bmatrix} \begin{bmatrix} V_{C1} \\ V_{C2} \\ i_L \end{bmatrix} + \begin{bmatrix} \frac{-i_L}{C} & \frac{i_L}{C} & 0 \\ 0 & \frac{-i_L}{C} & \frac{i_L}{C} \\ \frac{V_{C1}}{L_L} & \frac{V_{C2}-V_{C1}}{L_L} & \frac{V_{dc}-V_{C2}}{L_L} \end{bmatrix} \begin{bmatrix} S_1 \\ S_2 \\ S_3 \end{bmatrix} \tag{6}$$
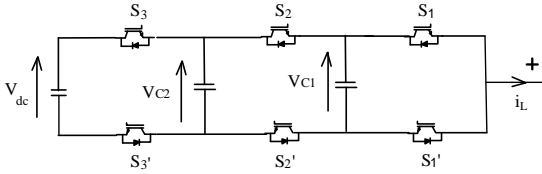

Fig. 1. Proposed system structure

Fig 2. Multicellular topology of power converter

2.1. Sliding mode control

İn references [11][18], the sliding mode control is used and assure the robustness and stability of multicellular converter. Therfore, in this paper the sliding mode control is applied in order to assure an efficient fault tolerant diagnosis ant fault tolerant control.

According to the Equation (6), the mathematical model of proposed topology power converter can expressed by the Equation (7):

$$\dot{x}=f(x)+g(x)u \qquad (7)$$

With

$x=[V_{C1}, V_{C2}, i_L]^T$ state vector.

$x_{ref}=[\frac{V_{dc}}{3}, \frac{2V_{dc}}{3}, i_L]^T$ reference vector.

$$f(x)=\begin{bmatrix} 0 & 0 & 0 \\ 0 & 0 & 0 \\ 0 & 0 & \frac{-R_L}{L_L} \end{bmatrix}, g(x)=\begin{bmatrix} \frac{-i_L}{C} & \frac{i_L}{C} & 0 \\ 0 & \frac{-i_L}{C} & \frac{i_L}{C} \\ \frac{V_{Cl}}{L_L} & \frac{V_{C2}-V_{Cl}}{L_L} & \frac{V_{dc}-V_{C2}}{L_L} \end{bmatrix}$$

$u=[S_1 S_2 S_3]^T$ input vector,

The sliding mode surface (Sr) is given by:

$Sr = x - x_{ref}$

The stability of proposed control is assured by Lyapunov approach

The Lyapunov function is expressed byEquation (9):

$$V=\frac{1}{2}Sr^2(x) \qquad (9)$$

The deriving of Lyapunov function is given in Equation (10):

$$\dot{V}=Sr(x)\dot{Sr}(x) \qquad (10)$$

The deriving of sliding surface in Equation (11):

$$\dot{Sr} = \dot{x} - \dot{x}_{ref} \qquad (11)$$

Substitute of Equation(7) in Equation (12) give the following equation

$$\dot{Sr}=f(x)+g(x)u-\dot{x}_{ref} \qquad (12)$$

The input control u is given in Equation (13)

$$u=u_{eq}+u_n \qquad (13)$$

Suppose an ideal sliding motion. This can be expressed as Sr(x)=0 and $\dot{Sr}$(x)=0.

$$u_{eq}=-(g(x))^{-1}(f(x)+H-\dot{x}_{ref}) \qquad (14)$$

$$u=-(g(x))^{-1}(f(x)+H-\dot{x}_{ref}) + u_n \qquad (15)$$

Substitution of Equation (16) in equation (13) gives the sliding surface with the following form (Equation (17)):

$$\dot{Sr}=g(x)u_n \qquad (16)$$

The deriving of LYAPUNOV function is given in Equation (18):

$$Sr(x)\dot{Sr}(x)=Sr(x)g(x)u_n \qquad (17)$$

So the Equation (18) can be expressed in Equation (19) of

$$Sr(x)\dot{Sr}(x) = Sr(x)\left[\left(\frac{i_L}{C} + \frac{V_{C1}}{L_L}\right)u_{n1} \right.$$
$$+ \left(\frac{i_L}{C} - \frac{i_L}{C} + \frac{V_{C2} - V_{C1}}{L_L}\right)u_{n2} \qquad (18)$$
$$\left. + \left(\frac{i_L}{C} + \frac{(V_{dc} - V_{C2})}{L_L}\right)u_{n3}\right]$$

To assure the stability according to LYAPUNOV approach, the following condition must be satisfied:

$$\dot{V}(x)<0 \qquad (19)$$

According to the Equation (18) andEquation (19), the sliding modeinputs are given in Equation (20):

$$u_{n1}=-\text{sign}\left[Sr(x)\left(\frac{i_L}{C} + \frac{V_{C1}}{L_L}\right)\right]$$

$$u_{n2}=-\text{sign}\left[Sr(x)\left(\frac{i_L}{C} - \frac{i_L}{C} + \frac{V_{C2} - V_{C1}}{L_L}\right)\right] \qquad (20)$$

$$u_{n3}=-\text{sign}\left[Sr(x)\left(\frac{i_L}{C} + \frac{(V_{dc} - V_{C2})}{L_L}\right)\right]$$
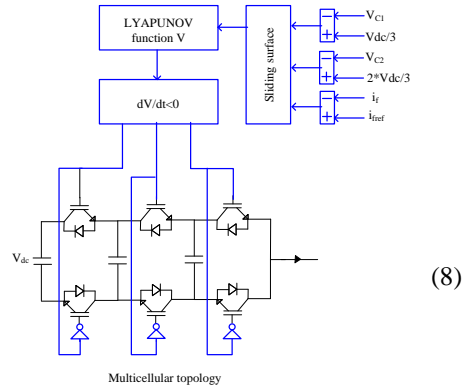
Figure 3 shows the sliding mode control algorithm.

(8)

Fig. 3. Sliding mode control algorithm

3. FAULT DIAGNOSIS METHOD

The fault diagnosis method includes the following steps:

- **Data analysis:** this step is used in order to differentiate between healthy operation mode and each of the failure modes, using feature space of figure 13. This later is based on 2 axes: voltage of capacitor C1 and voltage of capacitor C2. These axes are defined based on the physical knowledge about the behaviour of multicellular converter.

- **Classifier learning:** The aim of this step is to define a classifier able to assign a new pattern representing the operation conditions in the classes of feature space. These classes represent the faulty modes (failure of C1 and C2 and failure both C1 and C2) and healthy mode, and occupy restricted zones in the feature space (see Figure. 4). In order to build this classifier, a learning set is used and formed by historical data points about faulty operation modes and healthy mode. Each data point is represented as a pattern in the feature space and is defined by the voltage of two capacitors. In this work, we use the dynamic

classification method Fuzzy Pattern Matching (FPM)

- **Fuzzy Pattern Matching (FPM)**

a method based supervised classification to calculate the histogram probability and estimate the conditional probability density margin of all classes according to each attribute. with $K_1, K_2, ... , K_c$ are the classes described by d attributes. The attributes provide different points of view about the membership of an incoming pattern in the different classes. Two phases in FPM: the learning and the classification ones.

In this phase, the histograms probability is built for all class according to each attribute. Experimentally, determining the number of bins h for a histogram. The greatest lower and least upper boundaries of histogram can be considered as a maximal and minimal training data coordinates or by experts. The greatest of each bin b_k^j, $k \in \{1, 2, ... , h\}$, for each attribute j is the number of training patterns $n_{ib_k^j}$ of the class C_i located in this bin. The probability distribution
$\left\{ P_i^j \left(y_{b_k^j} \right), k \, \epsilon \{1, 2, ..., h\}, j \epsilon \{1, 2, ..., d\} \right\}$ of C_i class, $i \epsilon \{1, 2, ..., c\}$ with the attribute j is obtained by dividing the greatest of each bin by Ni (the total of training patterns) belonging to the same class C_i. equation (21).

$$P_i^j \left(y_{b_k^j} \right) = \frac{n_{ib_k^j}}{N_i} \qquad (21)$$

A linear interpolation between bins heights at their centers is used to obtain the probability density function (PDF). superior and inferior bins of height zero are added to each histogram probability. So, the goal is to link the centers of the first and last bins to zero (see Fig. 4). When a large number of data is available, the histogram can be assumed to approximate the PDF
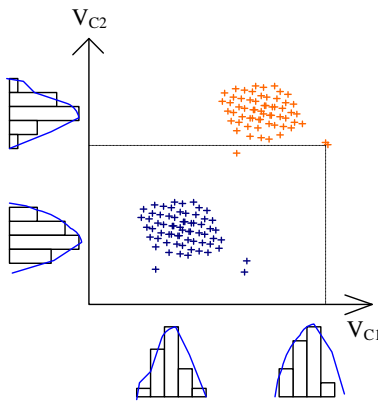

Fig. 4. Fuzzy pattern matching

The imprecision and the uncertainty contained in the data are taken in account, the probability distribution is converted into possibility one
$\left\{ \pi_i^j \left(y_{b_k^j} \right), k \, \epsilon \{1, 2, ..., h\}, j \epsilon \{1, 2, ..., d\} \right\}$. Based on the notion of a fuzzy set, Possibility theory was introduced in order to model and handle the uncertainty induced by pieces of vague or imprecise linguistic information. Using the transformation of Dubois and Prade [24] The conversion of probability into possibility is performed as the following equation (22)

$$\pi_i^j \left(y_{b_k^j} \right) = \sum_{f=k}^{h} \min \left(p_i^j \left(y_{b_k^j} \right), p_i^j \left(y_{b_f^i} \right) \right) \qquad (22)$$

The membership function $\{\pi_i^j, i \in \{1,2,\ldots,c\}, j \in \{1,2,\ldots,d\}$, is estimated for each class *i* according to each feature *j*. These membership functions allow assigning a pattern to a class as follows. The membership value $\pi_i^j(x)$ of a pattern *x* to the class *i* according to a feature *j* is calculated by projecting *x* into π_i^j. Then, the membership values $\pi_i^1(x), \pi_i^2(x), \ldots, \pi_i^d(x)$ of x to the class i according to all features *j* = 1, ..., d, are fused using the aggregation operator "minimum' in order to obtain the membership π_i^j of x to the class *i*. The membership values $\pi_1(x), \pi_2(x), \ldots, \pi_c(x)$ of *x* to all the classes are then calculated. *x* will finally be assigned to the class for which it has the highest membership value. More details about the functioning of this method can be found in [16] and the references therein. This method was used because it is simple and has a low and constant classification time according to the size of the database [24].

4. RESULTS OF SIMULATION STUDIES

Simulation parameters are summarized in table 1.
All power switches have ideal operating and all figures are obtained with Matlab software.

Table 1. Simulation parameters

Parameter	Value
V_{dc}	270V
R_L and L_L	15Ω and 2mH
C	40μF

- **Healthy mode operating**
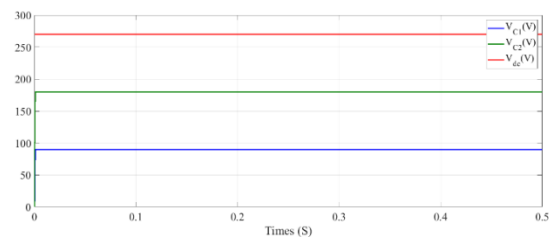 The feature spaces are between V_{C1} and V_{C2}

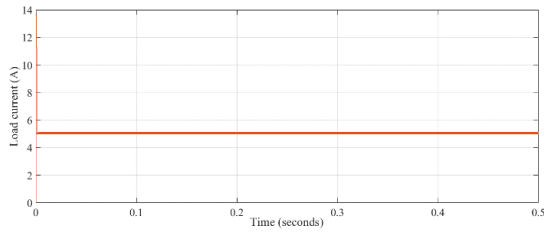Fig. 5. DC voltage and flying capacitor voltages in healthy mode

Fig. 6. Load current healthy mode

In healthy operating mode (Figure 5) the voltages of flying capacitors equal to their desired values in steady state. The load current (Figure 6) equal to desired value 5A.

- **Healthy mode with load variation**

In order to test the quality of sliding mode, a variation of load resistor from 15Ω to 3Ω at 0.2s. The results are shown in figures 7 and 8. These results proves the robustness of sliding mode against load variations.
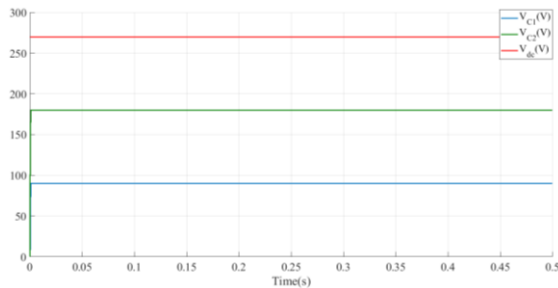

Fig. 7. dc voltage and flying capacitor voltages in healthy mode with load variation
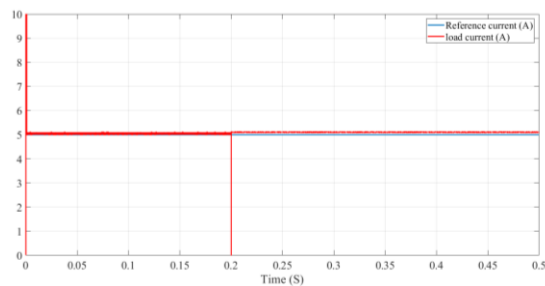
Fig. 8. Load current healthy mode with load variation

- **Healthy mode with reference current variation**

In this test of robustness, the reference current is changed from 5A to 10A at 0.2s (figure 9). These result proves the robustness of proposed control.
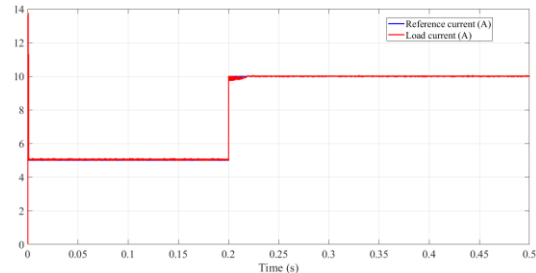

Fig. 9. Load current healthy mode with reference current variation

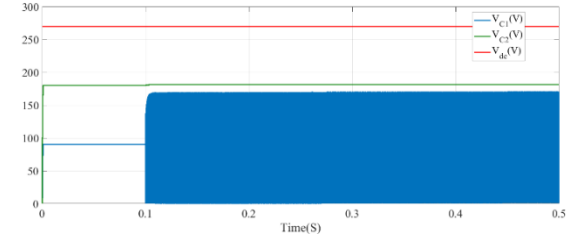- **Failure of capacitor C1**

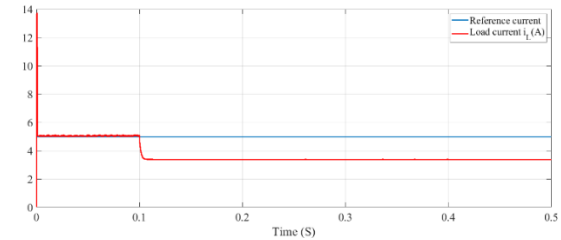Fig. 10. DC voltage and flying capacitor voltages in C1 failure mode

Fig. 11. Load current in C1 failure mode

When C1 is broken the voltage V_{c1} deviates from the desired value (Figure 10) and the static error of voltage V_{c2} is increased.

The load current (Figure 11) deviates from its reference and the static error of load current equal to 1.5A
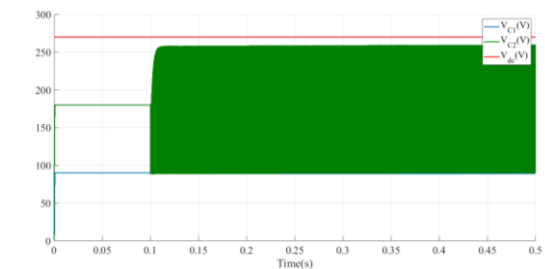
- **Failure of capacitor C2**

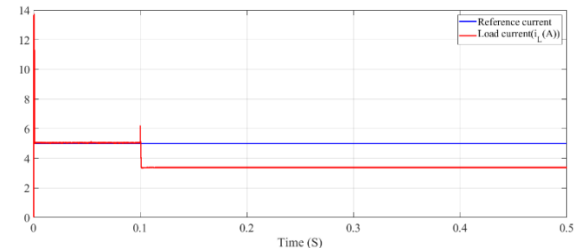Fig. 12. dc voltage and flying capacitor voltages in C2 failure mode

Fig. 13. Load current in C2 failure mode

If C2 is broken the voltage V_{c2} deviates from the desired value (Figure 12) and the static error of voltage V_{c1} is increased. The load current (Figure 13) deviates from its reference and the static error of load current equal to 1.5A.
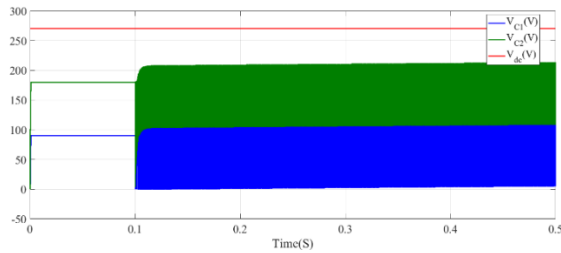
- **Failure of capacitors C1 and C2**

Fig. 14. DC voltage and flying capacitor voltages in C1 and C2 failure mode
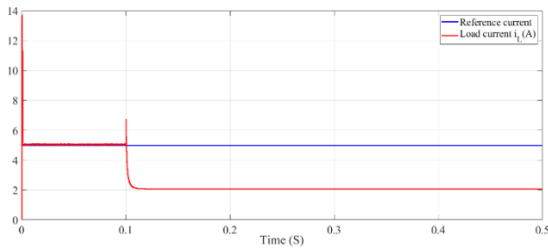

Fig. 15. Load current in C1 and C2 failure mode

When C1 and C2 are broken the voltage V_{c1} and V_{c2} deviate from their desired values (Figure 14).

The load current (Figure 15) deviates from its reference and the static error of load current equal to 3 A

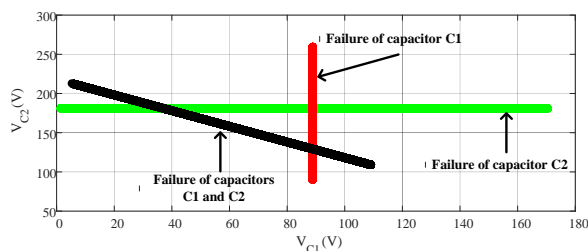Figure 16 shows the feature space of different operating mode.

Fig. 16. feature space of different operating mode

Using a computer with Intel (R) Core(TM) i5 and 2.50 GHz, The FPM classification time for each pattern (the detection, integration and adaptation online) is equal to $3*10-1$ second. These results prove the effectiveness and efficiency of proposed algorithm.

5. CONCLUSION

This work presented a multicellular converter used in aircraft system with robust sliding mode control and fault diagnosis strategy using FPM. and fault tolerant control using second multicellular converter. This structure assured the continuity and safety operating in electric parts of more electric aircraft, as well as increase the robustness. when a failure in capacitors of multicellular converter occurred, load current and capacitor voltage deviated from their references, which increase mechanical vibrations and heat stress. The FPM algorithm detect the failure mode from used feature space than the second multicellular converter is working until the

arrival of maintenance team. Simulations with software MATLAB/ Simulink proved the effectiveness of the proposed fault diagnosis method with reduced time to eliminate the failure impact on the aircraft system; this can prevent the propagation of failure to other healthy parts of electric system and increase the lifetime of aircraft.

As further direction, we propose to deal with fault prognosis and remaining useful life (RUL) estimation in more electric aircraft.

Author contributions: *research concept and design, M.A.M., M.R.K., H.T.; Collection and/or assembly of data, M.A.M., M.R.K., H.T.; Data analysis and interpretation, M.A.M., B.R., M.R.K., H.T.; Writing the article, M.A.M., B.R., M.R.K., H.T.; Critical revision of the article, B.R.; Final approval of the article, B.R., H.T.*

Declaration of competing interest: *The authors declare that they have no known competing financial interests or personal relationships that could have appeared to influence the work reported in this paper.*

REFERENCES

1. Rodger D. Current status and future plans for electric motors and drives at NASA. IEEE International Electric Motors and Drives Conference. 2021.
2. Simons DG, Besnea I, Mohammadloo TH, Melkert JA, Snellen M. Comparative assessment of measured and modelled aircraft noise around Amsterdam Airport Schiphol. Transportation Research Part D: Transport and Environment. 2022;105:103216. https://doi.org/10.1016/j.trd.2022.103216.
3. Yang J, Buticchi G, Gu C, Wheeler P. Impedance-based stability analysis of permanent magnet synchronous generator for the more electric aircraft. 2021 IEEE Workshop on Electrical Machines Design, Control and Diagnosis (WEMDCD). 2021:181-185. https://doi.org/10.1109/WEMDCD51469.2021.9425679.
4. Benzaquen J, He J, Mirafzal B. Toward more electric powertrains in aircraft: Technical challenges and advancements. CES Transactions on Electrical Machines and Systems. 2021;5(3):177-193. https://doi.org/10.30941/CESTEMS.2021.00022.
5. Cavallo A, Canciello G, Russo A. Integrated supervised adaptive control for the more electric aircraft. Automatica. 2020;117. https://doi.org/10.1016/j.automatica.2020.108956.
6. Wheeler, P, Bozhko, S. The more electric aircraft: Technology and challenges. IEEE Electrification Magazine. 2014; 2(4):6–12. https://doi.org/10.1109/mele.2014.2360720.
7. Cheryl B. Visions of the Future: Hybrid Electric Aircraft Propulsion. AIAA Aircraft Electric/Hybrid-Electric Power & Propulsion Workshop, National Aeronautics and Space Administration NASA. 2016.
8. Gębura A. Four models of tribological wear of turbine jet engine bearings based on methods of electrical generator signal analysis. Diagnostyka. 2017;18(1): 59-66.

9. Kumar BVR, Sivakumar K, Reddy KM, Karunanidhi S. A new fault tolerant dual rotor BLDC drive for electro-mechanical actuator in more electric aircraft applications. 2017 IEEE Transportation Electrification Conference ITEC-India. 2017:1-4, https://doi.org/10.1109/ITEC-India.2017.8356944.

10. Rouabah B. Contribution à l'amélioration des performances d'un filtre actif parall`ele de puis- sance par l'utilisation d'un convertisseur multicel- lulaire. PhD dissertation. Universit´e Ferhat ABBAS - S´etif; 2021. http://dspace.univ-setif.dz:8888/jspui/handle/123456789/3803.

11. Rouabah B, Rahmani L, Mahboub H, Toubakh MA, Mouchaweh MS. More efficient wind energy conversion system using shunt active power filter. J Electr Power Compon Syst 2021. https://doi.org/10.1080/15325008.2021.1970285.

12. Rouabah B, Rahmani L, Toubakh H, Duviella E. Adaptive and exact linearization control of multicellular power converter based on shunt active power filter. J Control Autom Electr Syst. 2019. https://doi.org/10.1007/s40313-019-00510-w.

13. Defaÿ M, Llor AM, Fadel M. A predictive control with flying capacitor balancing of a multicell active power filter. IEEE transactions on industrial electronics 2008; 55: 3212-3220.

14. Ben Said S, Ben Saad K, Benrejeb M. HIL simulation approach for a multicellular converter controlled by sliding mode. International Journal of Hydrogen Energy. 2017;42(17):12790–2796. https://doi.org/10.1016/j.ijhydene.2017.01.198.

15. Houari Toubakh, Moamar Sayed-Mouchaweh, Eric Duviella. advanced pattern recognition approach for fault diagnosis of wind turbines. 12th IEEE International Conference on Machine Learning and Applications. ICMLA, 2013: 368- 37

16. Houari Toubakh, Moamar Sayed-Mouchaweh, Anthony Fleury, Jacques Boonaert. Hybrid dynamic data mining scheme for drift-like fault diagnosis in multicellular converters. IEEE 2015: 56-61

17. Houari Toubakh, Moamar Sayed-Mouchaweh. Hybrid dynamic classifier for drift-like fault diagnosis in a class of hybrid dynamic systems: Application to wind turbine converters. Neurocomputing Journal 2016. https://doi.org/10.1016/j.neucom.2015.07.073.

18. Boubakeur Rouabah, Houari Toubakh, Moamar Sayed-Mouchaweh, Fault tolerant control of multicellular converter used in shunt active power filter. Electric Power Systems Research. 2020;188:106533. https://doi.org/10.1016/j.epsr.2020.106533.

19. Roubah B, Toubakh H, Sayed M. Advanced fault-tolerant control strategy of wind turbine based on squirrel cage induction generator with rotor bar defects. Annual Conference of the Prognostics and Health Management (PHM) Society 2019. https://doi.org/10.36001/phmconf.2019.v11i1.841.

20. Tokarski, TH. Evaluation of direct current electric power systems of the aircraft based on characteristics of a transient state. Diagnostyka, 2019;20(1):81-91. https://doi.org/10.29354/diag/100439.

21. Umair Ahmed, Fakhre Ali, Ian Jennions, A review of aircraft auxiliary power unit faults, diagnostics and acoustic measurements. Progress in Aerospace Sciences. 2021;124. https://doi.org/10.1016/j.paerosci.2021.100721.

22. Sayed Mouchaweh M. Semi-supervised classification method for dynamic applications. Fuzzy Sets and Systems. 2010;161(4):544–563. https://doi.org/10.1016/j.fss.2009.11.002.

23. Boubakeur Rouabah, Houari Toubakh, Mohamed Redouane Kafi, Moamar Sayed-Mouchaweh. Adaptive data-driven fault-tolerant control strategy for optimal power extraction in presence of broken rotor bars in wind turbine, ISA Transactions. 2022, https://doi.org/10.1016/j.isatra.2022.04.008.

24. Moamar Sayed Mouchaweh, Arnaud Devillez, Gerard Villermain Lecolier, Patrice Billaudel. Incremental learning in Fuzzy Pattern Matching. Fuzzy Sets and Systems. 2002;132(1). https://doi.org/10.1016/S0165-0114(02)00060-X.

Mohamed Abdelbasset MAHBOUB Received his Engineer from University of setif in 2009, Magister from university of Setif, Algeria in 2012, and PhD from university of Batna algeria in 2017. In 2019 until now, he was a researcher at University of Kasdi Merbah Ouargla, Algeria.

Boubakeur ROUABAH Received his Engineer from University of Bordj Bou Arriridj in 2009, Magister from university of Setif, Algeria in 2012, and PhD from university of setif-1 Algeria in 2021. In 2020 until now, he was a researcher at University of Kasdi Merbah Ouargla, Algeria.

Mohamed Redouane KAFI currently works at the Department of Electrical Engineering, Université Kasdi Merbah Ouargla. Kafi does research in Aeronautical Engineering, Control Systems Engineering and Electronic Engineering.

Houari TOUBAKH Received his Engineering Degree in Electrical Engineering from the University of Technology, Setif, Algeria, in 2010. Then, he received his Master Degree in Automatical and Computer Engineering from the National Polytechnic Institute of Marseille France in 2012. He is curently Ph.D student in the High National Engineering School of Mines "Ecole Nationale Supérieure des Mines de Douai" at the Department of Automatic Control and Computer Science (Informatique & Automatique IA). His research interests include machine learning, wind turbine, diagnosis and prognosis of industrial production system using artificial intelligence techniques.